

PRECIPITATION AMOUNTS TRIGGERING LANDSLIDE PROCESSES IN THE WESTERN PART OF THE NAŁĘCZÓW PLATEAU (LUBLIN UPLAND, POLAND)

PIOTR DEMCZUK ¹, TYMOTEUZ ZYDRÓN ², TOMASZ SZAFRAN ³

¹ Institute of Earth and Environmental Sciences, Maria Curie-Skłodowska University in Lublin, Lublin, Poland

² Department of Hydraulic Engineering and Geotechnics, University of Agriculture in Kraków, Kraków, Poland

³ Lublin Landscape Parks Unit, Chełm, Poland

Manuscript received: January 31, 2022

Revised version: May 28, 2022

DEMCZUK P., ZYDRÓN T., SZAFRAN T., 2022. Precipitation amounts triggering landslide processes in the western part of the Nałęczów Plateau (Lublin Upland, Poland). *Quaestiones Geographicae* 41(3), Bogucki Wydawnictwo Naukowe, Poznań, pp. 33–51. 14 figs, 3 tables.

ABSTRACT: This study covers the western part of Poland's loess Nałęczów Plateau (Kazimierz Dolny, Zbędowice). Mass movements in the Lublin Upland occur during periods of increased precipitation or after a snowy and cold winter. To date, there are no comprehensive studies on active (precipitation, hydrology, vegetation, land use, anthropogenic factors) or passive factors (lithology, slope angle) causing such geohazards in this region. This area's formations are characterised by high sensitivity to even small changes in moisture content; thus, their geotechnical parameters deteriorate as a result of precipitation or rising groundwater levels. The calculations in this study were chosen to determine the time necessary for ground response to external factors, in addition to determining the impact of these factors on decreases in the factor of safety (FS). Based on calculations in GeoStudio software, the impacts of rainfall totals and duration on slope failure, interpreted as an event where the FS falls below 1.0, were analysed. Accordingly, the threshold rainfall value was determined as the total rainfall at the time of slope failure. The study's results indicate that loess covers are characterised by average water permeability, relatively high internal friction angles and low cohesion, which, combined with high slope inclination, favour landslide formation even when the slope is only partially saturated. The most unfavourable stability conditions occur at the beginning of spring, indicating that loess stability is significantly affected by snowmelt and precipitation at the beginning of the vegetation season, as well as the occurrence of episodic intense precipitation during the summer.

KEY WORDS: slope stability, shallow landslide, rainfall thresholds, loess, the Nałęczów Plateau

Corresponding author: Piotr Demczuk, piotr.demczuk@mail.umcs.pl

Introduction

There has been increasing interest in landslide processes in recent years, mainly in connection with the formation and activation of landslides in Poland following the floods in 1997 (German 1998, Poprawa, Rączkowski 1998, 2003, Oszczypko et al. 2002) and after the 2010 flooding

events (Kaczmarczyk et al. 2011, Wysokiński 2011). Most ongoing research programmes are limited to short, one-off flooding events, surface measurements and mapping (Rybicki et al. 1998, Rączkowski, Mrozek 2002, Dziewański et al. 2004, Gorczyca 2004). A major component of these studies focuses on large structural landslides involving deep-seated Neogene, Paleogene

and older rocks while neglecting shallow landslides that occur at the boundary between eluvium and solid rock, as well as those occurring within the eluvium itself. According to SOPO (Landslide Protection System), around 50% of Carpathian landslides are ground and eluvium landslides. In contrast, in other parts of Poland, outside the Sudety area, most mass movements occur mainly within the ground. Given climate change predictions in future years, shallow mass movements are expected to intensify in Europe, with a decreased proportion of structural landslides (Gariano, Guzzetti 2016).

The major factors contributing to landslide susceptibility are generally divided into passive and active types. Passive factors include lithology and slope inclination, whereas active factors are precipitation, changing land use, hydrology, seismic and para-seismic earthquakes and anthropogenic effects. Presently, precipitation and the erosion of riverbanks and watercourses are considered to be the main factors contributing to landslide initiation. Thus, one of the most important tasks faced by contemporary landslide researchers is determining the precipitation thresholds triggering the formation of new landslides and the reactivation of old ones and, on this basis, developing an early warning system for mass movements (Segoni et al. 2014, Calvellido et al. 2015, Gariano et al., 2015, Chae et al. 2017, Lee et al. 2020, Abraham et al. 2021).

Precisely determining these precipitation thresholds requires knowledge not only of the nature of precipitation in a given area but also its geology and geomorphology, climate conditions and temporal and spatial variability of landslide formation conditions. Determining the critical precipitation levels for landslide triggering consists of:

- identifying the relationship between accumulated precipitation and precipitation duration (associated with landslide formation); and
- identifying the minimum value of the precipitation threshold (at which landslides start forming). This is equivalent to describing the relationship between rainfall and activation of the slope cover (Demczuk et al. 2019).

The study covers the western part of the loess Nałęczów Plateau, in the vicinity of Kazimierz Dolny and Zbędownice, Poland. In terms of

mass movement studies, this area represents a white spot only discussed in occasional publications (e.g. Harasimiuk et al. 2000, Borecka, Kaczmarczyk 2007, Rodzik et al. 2008). Mass movements in the Lublin Upland occur during times of increased precipitation or after a cold and snowy winter; however, to date, there are no comprehensive studies on the active and passive factors causing such geohazards in this region. The high landslide potential of the area is evidenced by SOPO data and landslide susceptibility maps (Wojciechowski 2019). Research results and examples of building failures in areas with loess cover from various regions indicate that this deposit type is susceptible to denudation processes, including mass movements. In general, due to the nature of their genesis, these formations are characterised by high sensitivity to even small changes in moisture content and their geotechnical parameters thus deteriorate as a result of precipitation or rising groundwater levels (Teisseyre 1994, Higgins and Modeer 1996, Mularz et al. 1999, Borecka, Kaczmarczyk 2007, Tu et al. 2009, Xu et al. 2012, 2018, Zhou et al. 2014, Yates et al. 2018, Shi et al. 2020, Leng et al. 2021, Xie et al. 2021, Zhu et al. 2021).

Due to the lack of precise data on landslide formation in the western part of the Nałęczów Plateau and, thus, the impossibility of determining threshold precipitation levels by empirical means, a deterministic method based on analysis of physical phenomena in the landslide slope profile after precipitation is used in this study. This approach considers the characteristics of a given slope, its retention characteristics, the flow and accumulation of water in the slope cover, changes in stress force occurring in the slope profile, decreases in frictional resistance and the physical properties of the slope-forming material (Demczuk et al. 2019).

The planned calculations were intended to determine the time necessary for the ground (i.e. slope failure) to react to external factors (e.g. precipitation, ground cover), as well as determine the effects of these factors on decreases in the factor of safety (FS). These calculations thus provide insights into the relationship between precipitation levels and their duration, which represent the basis for forecasting landslide hazard risks.

Study area

Geology and geomorphological characteristics

The studied sites are located in the vicinity of Zbędownice and Kazimierz Dolny, in the western part of the Nałęczów Plateau, Poland. The Nałęczów Plateau forms part of the Lublin Upland, stretching between the Vistula and Bystrzyca valleys, in a WNW–ESE direction. It forms a broad, flat bed rising 200–220 m a.s.l. (with a length of around 45 km and a width of 10–13 km). To the north and south, the region is a morphological edge. The bedrock of the western part of the Nałęczów Plateau is formed from a diverse range of fractured rocks of Maastrichtian and Palaeogene ages (Pożaryski 1948, Pożaryska 1967, Henkiel, Nitychoruk 1983, Abdel-Gawad 1986, Źarski et al. 1998, Machalski 2005). The topography of the sub-Quaternary basement in the Vistula region exceeds 150 m, decreasing to around 70 m towards the east (in the vicinity of

Wąwolnica) (Harasimiuk, Henkiel 1976). This deep bedrock topography was formed at the end of the Early Pleistocene in connection with the development of the Vistula Valley and its erosion. These features determine the contemporary structure of the valley network in the Nałęczów Plateau (Harasimiuk 1980, Henkiel, Nitychoruk 1983, Pożaryski et al. 1994) (Fig. 1).

In the Nałęczów Plateau, Pleistocene glacial, fluvioglacial and limnoglacial deposits from the Odra glaciation directly overlie sub-Quaternary rocks. North of the Bystra valley, the thickness of the glacial deposits exceeds 20 m. On the other side of the Bystra valley, boulder clay deposits form a thin, discontinuous cover. The formation of these sediments results from the location of this part of the Lublin Upland in the marginal zone of the Odra continental glacier in the post-maximal stadial (Fig. 2A) (Harasimiuk, Henkiel 1976, 1978, Źarski 1988, Pożaryski et al. 1994).

The youngest Pleistocene sediments are represented by a continuous loess cover from the Weichselian glacial period. These sediments

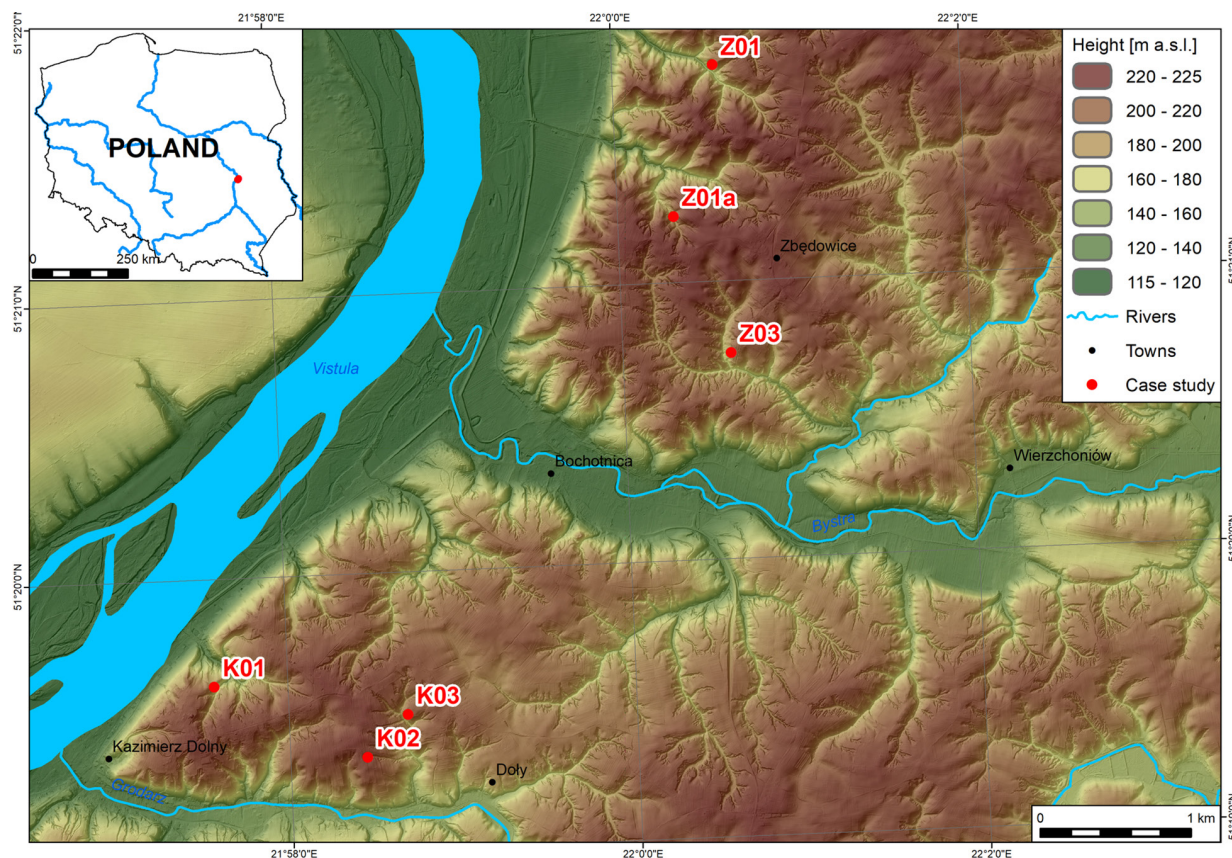


Fig. 1. Location of research sites shown against a LiDAR elevation-based shaded relief map of the western part of the Nałęczów Plateau.

originate from a uniform period of loess formation, which was preceded by several interstadial phases during which poorly developed, initial fossil soils were formed (Harasimiuk, Henkiel 1978, Maruszczak 1991). In the western part of the Nałęczów Plateau, the average depth of the loess cover is 15–20 m, while in the northern and

marginal areas of this region and along the valleys of the Bystra and Grodarz rivers, the loess depth reaches 30 m. This significant loess cover thickness results from the infill of depressions, valleys and pre-Quaternary valleys (Fig. 2B) (Harasimiuk, Jezierski 1998).

The relief of the Nałęczów Plateau is dominated by elements relating to loess cover thickness and the formation of loess subsoils. In the upper parts of the loess uplands, a network of valleys and undulating relief is observed in fine-grained deposits. In areas where the loess cover thickness exceeds 10 m, the relief is of a denudational subtype with low altitude differences (up to 30 m), shallow denudation basins and depressions without outflows. The denudation–erosion sculpture subtype appears in areas where the loess thickness reaches 15–20 m. These areas are characterised by altitude differences of up to 60 m and a dense network of erosion–denudation valleys. In contrast, in areas where the loess thickness reaches 30 m, an erosional relief subtype with a contemporary system of extensive systems of erosion–denudation valleys will develop. Altitude differences in these areas may reach up to 100 m and the network of valleys and top parts is cut by ravines whose density reaches up to $17.6 \text{ km} \cdot \text{km}^{-2}$ (mean = $8.6 \text{ km} \cdot \text{km}^{-2}$; own research based on LiDAR data). According to the data of Kęsik (1961), the density of gullies network ranges from $0.5 \text{ km} \cdot \text{km}^{-2}$ in the southern part of the Plateau to $5.0 \text{ km} \cdot \text{km}^{-2}$ between Kazimierz Dolny and Puławy in the north-western part of this region. Such strong incision of the western part of the Nałęczów Plateau is connected with the deep erosional base of the Vistula River (Fig. 2C) (Maruszczak 1973).

The presence of loess rocks as aeolian deposits, which are poorly cemented and porous (and thus susceptible to thawing and suffosion), in contact with low- and very low-permeability glacial sediments (boulder clays, proglacial clays) and steep ravine slopes of up to 50° , favours landslide formation processes.

Precipitation

Atmospheric precipitation is often the key factor driving slope instability processes. With time, precipitation is transformed into surface runoff and evaporation, with a part retained in the slope

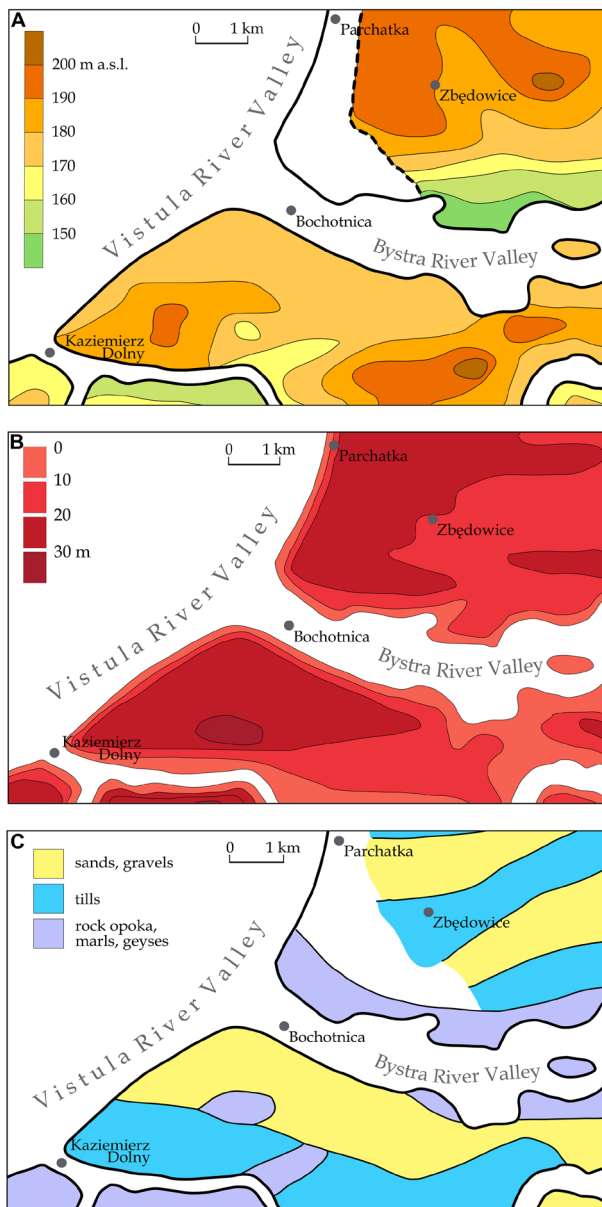


Fig. 2. Geological structure of the research area. A – Geological map of the sub-loess surface of the western part of the Nałęczów Plateau, with the study area marked by a red box (Harasimiuk, Henkiel 1975/1976), B – Hypsometric tints of the sub-loess surface of the western part of the Nałęczów Plateau, with the study area marked (Harasimiuk, Henkiel 1975/1976), C – Map of loess cover thickness in the western part of the Nałęczów Plateau with marked study area (Harasimiuk, Henkiel 1975/1976).

cover. The important features of precipitation, ultimately determining the occurrence or intensity of the associated processes, are its height, duration and intensity.

Close to the Nałęczów Plateau, there is one meteorological station from the Institute of Meteorology and Water Management in Puławy (IMGW) that has conducted meteorological observations since 1951. Until 2000, there was a precipitation station of the Institute of Meteorology and Water Management situated in Kazimierz Dolny; however, over 50 years, the data are only 55% complete. In addition, there are single observation stations located in the Plateau, but their observation periods do not exceed 10 years. Precipitation in the marginal zone of the Lublin Upland is characterised by large spatial and seasonal variability. In this area, precipitation is associated with diversified hypsometry, slope exposure and the presence of valleys of various sizes, as well as deep denudation and erosional valleys.

The meteorological station in Puławy is located close to the Nałęczów Plateau at an altitude

of 142 m a.s.l. The average total precipitation for the years 1951–2020 is 576.4 mm, with the highest annual precipitation level recorded in 1974 (797.3 mm) and the lowest recorded in the first observation year (1951) with 403.6 mm. According to Kaczorowska’s classification (1962), extremely dry years (i.e. below 50% of the long-term mean precipitation level, 289.2 mm) were recorded in the 70-year observation period. According to this classification, years with average precipitation (90–110% of the average precipitation) dominated, of which there were around 30. There were only 5 very wet years (126–150% of the average precipitation), namely, 1966, 1974, 1980, 2014 and 2017. Notably, these years are none of those in which catastrophic landslide events occurred in the Carpathians and Carpathian Foothills (Fig. 3).

Precipitation in the summer half-year (May–October) averaged 64% of the annual precipitation levels for 1951–2020. In this period, only two precipitation seasons differed in character, i.e. precipitation in the winter half-year (November–April) exceeded the summer (1967 and 1979). In 14 cases, the precipitation prevalence in the

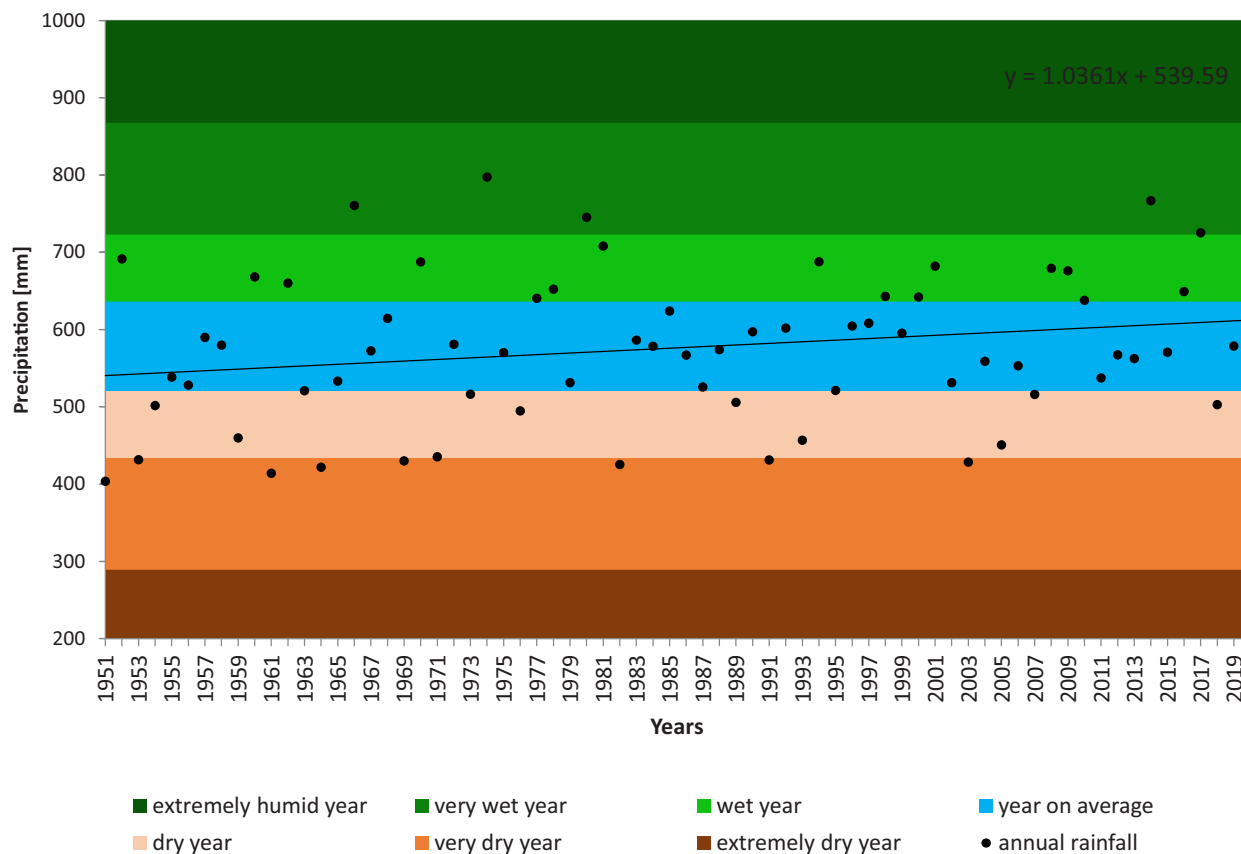


Fig. 3. Total annual precipitation for the years 1951–2020 at the IMGW station in Puławy plotted against the Kaczorowska classification (1962).

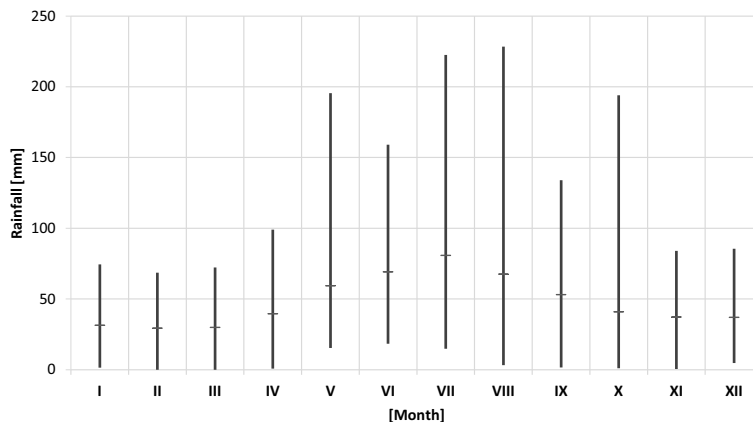


Fig. 4. Distribution of maximum, average and minimum monthly precipitation totals in the 1951–2020 period at the IMGW station in Puławy.

summer half-year exceeded 70%, with a maximum value of 80.5% recorded in 1974. Similarly, as in the case of precipitation in the summer and winter seasons, the precipitation amount recorded in climate seasons also fluctuated considerably. The summer season, from June to July, exhibited the highest seasonal sums of precipitation (37.8% on average). The lowest precipitation levels were observed in the winter season (December–February), accounting for 17% of the annual precipitation sum (Fig. 4).

The distribution of monthly mean precipitation levels at the Puławy station is marked by a distinct peak in July and August, with the mean sum exceeding 65 mm. The highest average precipitation sums were recorded in July (80.7 mm). The highest monthly precipitation sums were recorded in July 2006 and August 2011, with values of 228.4 mm and 222.5 mm, respectively (Fig. 4).

As shown in Figure 5, days without rainfall dominated in the period 1951–2020, during which time they accounted for more than 56% of the days of the year. Days with very weak (0.1–1.0 mm) and weak (1.0–5.0 mm) precipitation constituted 13.9% and 16.6% of the year, respectively. Moderate and heavier precipitation (>5.0 mm) accounted for 9.3% of the days of the year. During the study period, precipitation exceeding $20 \text{ mm} \cdot \text{day}^{-1}$ was recorded an average of 3.6 times $\cdot \text{year}^{-1}$. However, 1981 was an exception, with nine occasions when rainfall exceeded 20 mm. The maximum daily precipitation values were recorded in July 1962 (73.3 mm), May 2014 (68 mm) and May 2001 (63.5 mm).

The structure of atmospheric precipitation in the Nałęczów Plateau area was determined by

analysing precipitation sequences for the period between 1951 and 2020. The combination of at least 2 days with precipitation and a precipitation sum of $\geq 0.1 \text{ mm}$ were defined as a precipitation sequence. Above-average precipitation sequences were determined based on the analysis of the duration and total precipitation level that occurred within the sequence. Threshold values defining above-average precipitation sequences and precipitation sum were defined as values whose probability exceeded 10% (i.e. 90th percentile). Based on this criterion, four classes were identified:

- Class 1. Above-average precipitation with a relatively short duration.
- Class 2. Above-average precipitation of long duration.

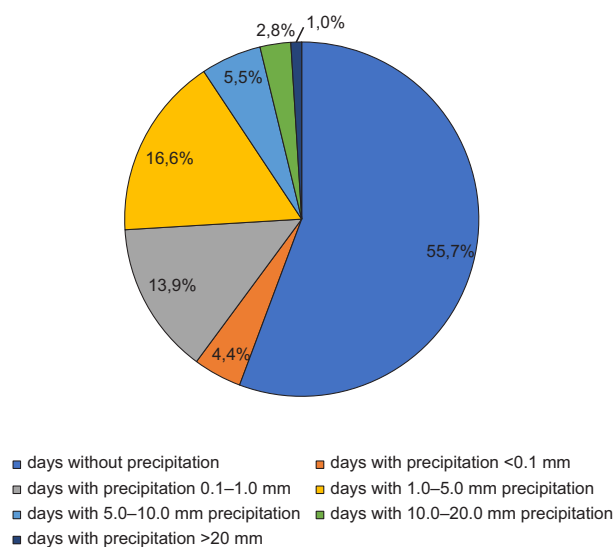


Fig. 5. Distribution of the average number of days with precipitation at various levels in the 1951–2020 period at the IMGW station in Puławy.

- Class 3. Prolonged precipitation of moderate magnitude.
- Class 4. Precipitation of short duration and moderate magnitude (Szalińska, Otop 2012).

During the study period (1951–2020), there were 2626 precipitation events lasting more than 1 day, of which 57% occurred in the period from April to October (1489 cases). The highest precipitation sum was 129.5 mm over 11 days (from 1 August to 11 August 2006). The longest precipitation sequence lasted 21 days (from 15 January to 4 February 1983), amounting to a total of 35 mm. In the warm period, the longest precipitation sequence lasted 16 days, with a sum of 63 mm. The highest number of recorded rainfall sequences fell in June and July, with average values of 18–20 mm.

From an analysis of all precipitation sequences taking place during the vegetation period (i.e. from April to October), the 90th percentile in precipitation duration was ascertained at 6 days, together with a precipitation sum of 38.8 mm. Class 2 precipitation, responsible for intensified surface runoff, flushing and initiation of landslide processes, occurred 54 times during the study period (3.8% of all precipitation sequences lasting longer than 1 day). The mean precipitation and duration values of this class were 63.2 mm and 9.4 days ($0.29 \text{ mm} \cdot \text{h}^{-1}$), respectively (Fig. 6).

The high precipitation period coincides with the vegetation season and the associated agro-technical cycle and lasts from April to September/

October. Apart from mountainous areas and the coastal zone, the Lublin Upland is characterised by numerous abrupt and heavy precipitation events, which may result from the climate being more continental in this part of Poland (Chomicz 1951, Maruszczak, Trembaczowski 1958, Parczewski 1960, Maruszczak 1986, Starkel 1986, 1996, 1997, 2008, Rodzik et al. 1998, 2008, Kaszewski, Siwek 2005, Siwek 2006, Kaszewski 2008, Lorenc et al. 2012). This part of the upland belt is also characterised upland by significant areas of high thermal and moisture contrasts, such as loess marginal zones, areas adjacent to zones of humid depressions or wide river valleys (the Vistula Valley), which generate downpours (Parczewski 1960, Rodzik et al. 1998, 2008, Rodzik, Janicki 2003).

Methodology

This study comprised field and laboratory tests, an analysis of precipitation in the study area and slope stability analyses. Field investigations included field mapping, survey measurements and geological drilling for the recognition of subsoil. Six slopes of various lengths were selected for analysis (Fig. 7). The land surveying measurements enabled the preparation of profiles through the studied landslides. The original shape of the analysed slopes was reproduced based on measurements in the nearby intact part

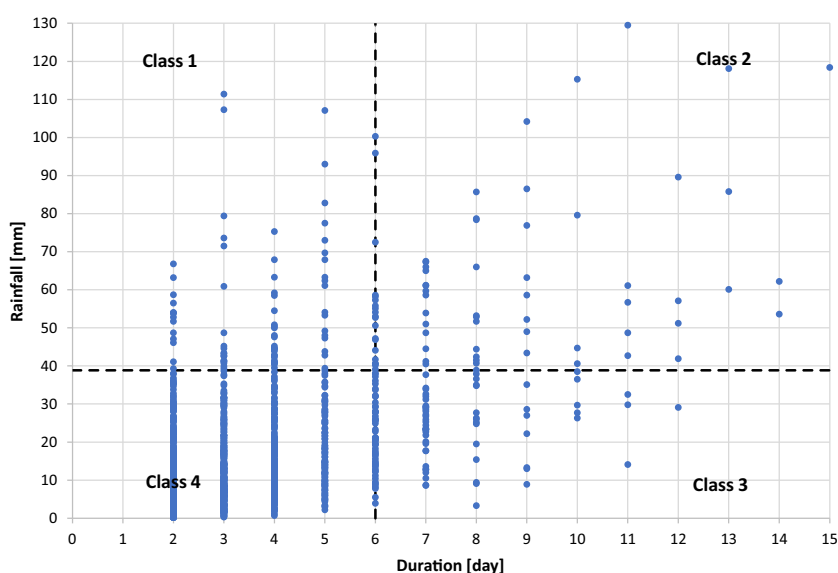


Fig. 6. Distribution of precipitation sequence lengths and totals in the 1951–2020 period at the IMGW station in Puławy.



Fig. 7. Photos of the slopes covered by the research.

of the slope and observations of outcrops of different soils in the valleys.

Boreholes were used to determine the lithology of the slopes and samples were taken for laboratory tests to determine their geotechnical parameters. In addition, soil permeability tests of surface formations and rocks comprising the slope were conducted in the field to a depth of 1.5 m below ground level. The laboratory tests comprised determining the soil moisture content, bulk density, Atterberg limits, soil permeability coefficient and effective values of shear strength parameters (i.e. angle of internal friction and cohesion). The shear strength was tested in a triaxial compression apparatus with sample saturation and application of the backpressure

technique until reaching a Skempton coefficient of at least 0.95 (Consolidated Isotropic Drained (CIU), Consolidated Isotropic Undrained (CID)). Soil permeability was tested in a triaxial compression apparatus. The laser diffraction method was used to determine the granulometric composition of the soils. Liquid limits were determined using the Cassagrande method.

Based on the land surveying and geotechnical tests, models of the slopes were prepared and slope stability analyses were then performed using GeoStudio software. This program enables the integration of seepage (Vadose/W, Seep/W) or dynamic stress distribution analysis (Quake/W) results with slope stability calculation (module Slope/W). This program is a tool

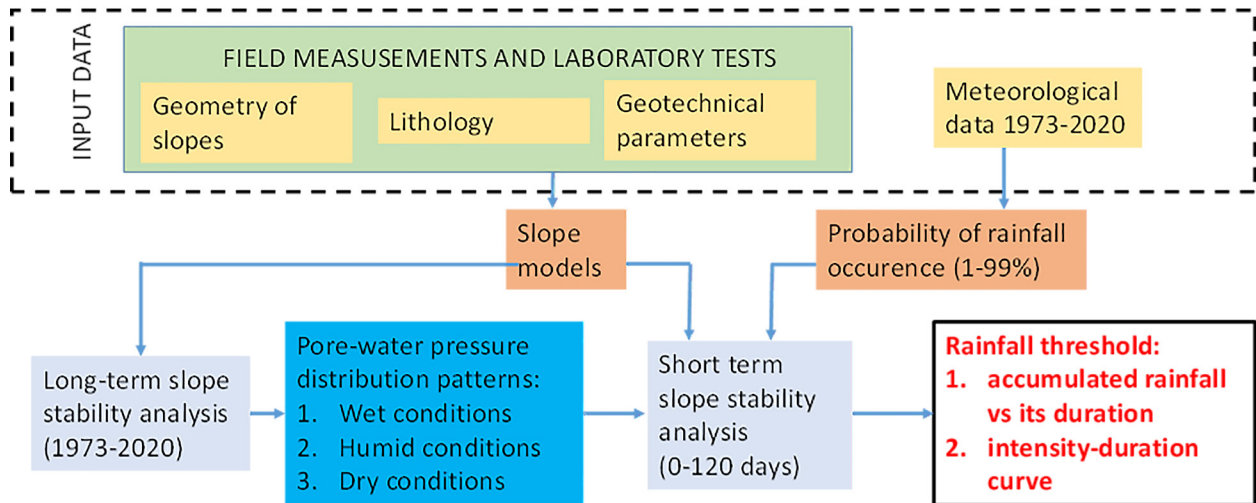


Fig. 8. Procedure for calculating the precipitation thresholds triggering landslides in the western part of the Nałęczów Plateau.

focused on typical engineering research but is rarely used in research by naturalists or geographers (Xu et al. 2013, Xiao-Li et al. 2016). The analysis was divided into two stages. In the first stage, calculations were made for each of the analysed slopes using meteorological data from the period 1973–2020 from the IMGW station in Puławy. The use of a shorter series of meteorological data (1973–2020) in the calculations in GeoStudio was due to incomplete data availability for air and ground temperature measurements. We used these calculations to determine extreme moisture content conditions within the ground during the analysed period. In addition, on this basis, we assumed three different initial soil moisture conditions for further slope stability calculations:

- dry, including a condition when there was no precipitation in the preceding period (August),
- humid, corresponding to the conditions of normal/most frequent soil moisture content in the warm half-year (May–October),
- wet, corresponding to a meteorological situation in which the period for which the analysis or calculation is performed was preceded by heavy rainfall and snowmelt (April).

In the second stage of analysis, we used these input moisture conditions' variants and determined the threshold precipitation sum for slope failure. As a factor contributing to changing slope stability, we considered 120-day precipitation periods of different occurrence probabilities. The

precipitation sum values with occurrence probabilities of 1, 2, 5, 10, 25, 50 and 99% and durations of 1–120 days were calculated using a logarithmic-normal distribution (Banasik et al. 2017). For each of these scenarios, we performed slope stability calculations using 120-day cumulative precipitation values with probabilities of occurrence of 1–99% and varying intensities (i.e. constant, increasing and decreasing). The slope stability calculations were performed using the Janbu method (limit equilibrium method). Among the many boundary equilibrium methods, the Janbu method usually gives the most pessimistic results, and the analysis included the values of the shear strength parameters at the maximum value of the stress deviator. Based on these calculations, the impacts of the rainfall totals and duration on slope failure, interpreted as an event where the FS reaches a value below 1.0, were analysed. In turn, the threshold rainfall value was determined as the total rainfall at the time of slope failure.

The overall scheme of the methodology used in this study is presented in Figure 8.

Results and discussion

Lithology and geotechnical characteristics of slopes

During geomorphological mapping of the western part of the Nałęczów Plateau, we mapped around 297 landslides (area of about

30 km²). However, these are preliminary results that may change with subsequent research. The average landslide density in the area is about 10 landslides · km⁻². The maximum intensity of landslides was identified in the Zbędownice area and exceeds the study area's average value by more than three times. The most common landslides are shallow turf landslides, where the thickness of the gravitationally displaced rock package does not exceed 50 cm, and whose area reaches up to 1 acre. In terms of surfaces, the largest landslides occur in areas with the thickest loess cover (typically over 10–15 m thickness),

lying on poorly permeable glacial till, where the depth of ravine slits is greatest. The intensity of landslide processes decreases with the upward movement of these valley forms - most landslides were observed on slopes of up to 35° (76% of the recorded landslides), with the highest intensity occurring on 25–35° slopes, accounting for 37% of the recorded landslides.

Six slopes in the vicinity of Kazimierz Dolny: Doły Podmularskie (K02, K03), Norowy Dół (K01)] and Zbędownice [Łachowy Dół (Z01a), on the road from Parchatka to Zbędownice (Z01), Szkutny Dół (Z03) were selected for analysis

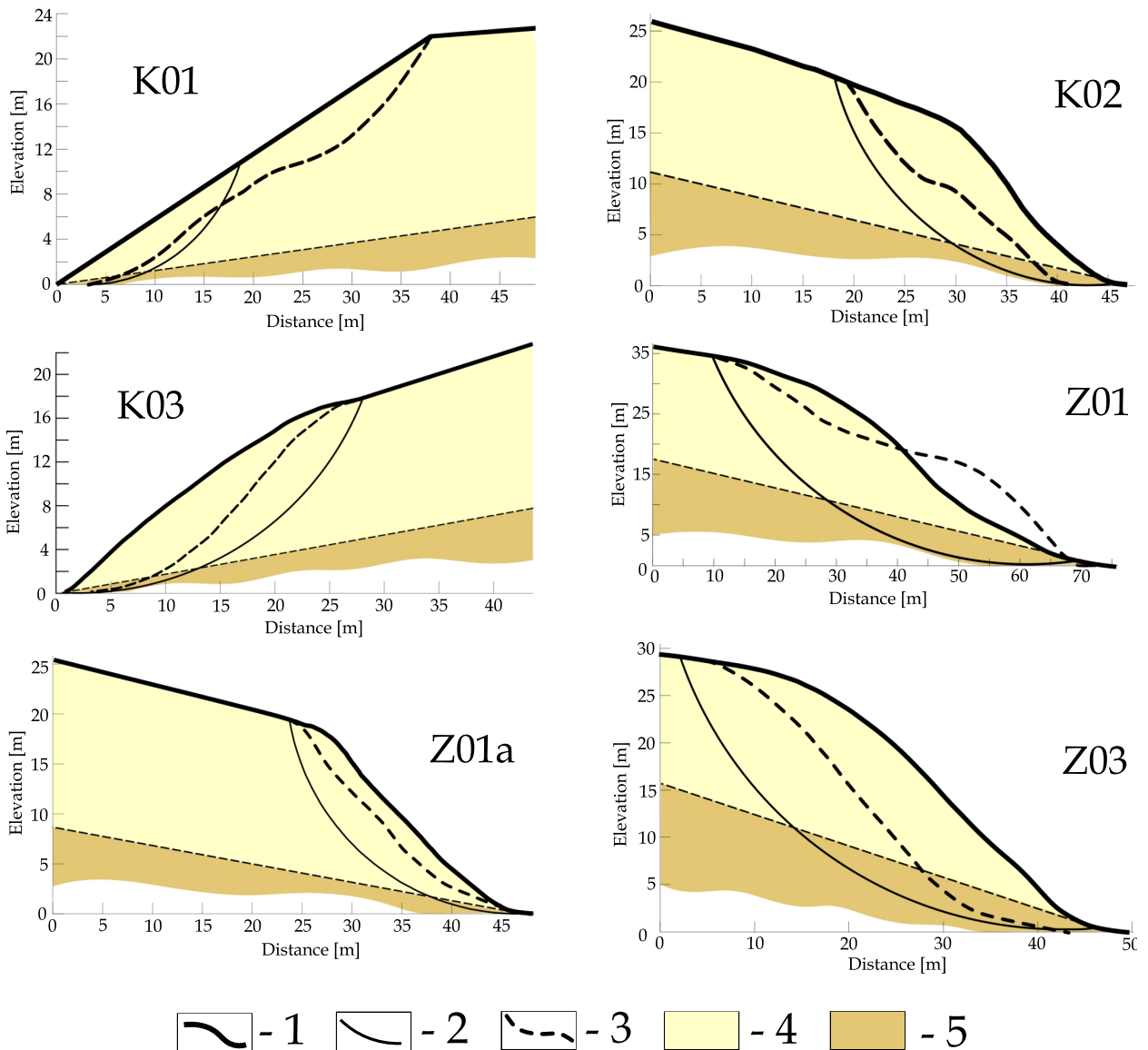


Fig. 9. Shape of reconstructed landslide slopes subjected to slope stability tests.

1 - assumed original slope shape, 2 - sliding surface, 3 - present slope shape, 4 - loess layer, 5 - layer with low water permeability.

Table 1. Parameters of research slopes.

Case study	Location [WGS84]		Slope	Length	Height	Thickness of colluvium	Landuse
	E [°]	N [°]	[°]	[m]			[%]
K01	21.95956	51.32689	30.0	120	21.0	7.7	Forest (100)
K02	21.974	51.32232	46.5	116	16.8	3.1	Forest (62), Fields (48)
K03	21.97799	51.32479	35.0	143	14.4	4.7	Forest (100)
Z01	22.00966	51.36299	36.5	255	36.6	7.9	Forest (50), Fields (50)
Z01a	22.00535	51.35397	45.0	190	16.8	5.6	Forest (74), Fields (26)
Z03	22.01034	51.34569	45.0	107	28.7	7.2	Forest (73), Fields (23)

(Table 1, Fig. 9). The selection of these study objects was based on literature analysis, environmental interviews with local inhabitants and geomorphological mapping of landslide formations in the western part of the Nałęczów Plateau. The selected slopes exhibited visible signs of landslide activity. They are located close to other landslide niches of various sizes, which are distinctly discernible from the surrounding region, and indicate that contemporary landslide processes have been in operation. The selected sites represent erosional ravine valleys with varying exposures and slopes, now shaped by the episodic flow of precipitation and snowmelt water. All the slopes are built of loess rocks with thicknesses varying from 15 m to 30 m (Vistula glaciation); in the lower parts of the profiles, clay sediments are identified, originating from the Odra glaciation period, or sandy/gravelly units underlie the loess (in the northern part of the research area). At the contact between the sedimentary rocks and glacial deposits, water effusions or zones of increased slope cover moisture were observed.

The results of our fieldwork show that the studied area experiences intense slope processes. These forms vary in size, with a significant proportion of the landslides being 20–40 m long and tending to occur in the lower part of the slopes, with visible zones of wetter soil in their vicinity. However, the boreholes did not reveal the presence of a shallow groundwater table.

Since the upper parts of the slopes were located in the vicinity of the landslides, the location of sliding surface (its entry and exit) was interpreted to coincide with the location of cracks, and colluvium thickness was ascertained based on the shape of intact slopes. Additionally, the Define Slip Surface Grid and Radius method from GeoStudio was used to determine the slip surface. This method is used to define the rotation centres and radii for circular and composite slip surfaces. To localise the position and inclination of the impermeable layer (e.g. clay layer), we identified its outcrops at the toe of the slope and in the beds of watercourses.

Table 2 contains the basic geotechnical parameters of the loess slope cover for each slope. The loess deposits from different sites exhibit very similar shear strength parameters and permeability coefficients, which is probably an effect of the highly consistent grain size distribution. These soils can be classified as silt and are characterised by medium permeability, relatively high internal friction angle values and very low cohesion, which are consistent with the results of loess studies from other regions (Xing et al. 2016, Xu et al. 2018).

Analysis of precipitation

Rainfall data from the vegetation seasons of 1951–2020 were used to determine the

Table 2. Main geotechnical parameters of loess cover at each site.

Case study	Angle of internal friction	Cohesion	Permeability	Fraction content			USDA	PN-EN ISO 14668-2:2006
	[°]			[kPa]	[m/s]	Clay		
				[%]				
K01	33.9	3.2	3.27×10^{-6}	6.4	67.0	26.6	silt loam	silt
K02	31.4	0.0	7.14×10^{-6}	5.4	66.2	28.4	silt loam	silt
K03	30.4	0.0	3.86×10^{-6}	4.8	61.4	33.8	silt loam	silt
Z01	31.2	0.0	2.20×10^{-6}	5.1	65.0	29.9	silt loam	silt
Z01a	34.3	0.0	2.36×10^{-6}	4.9	64.9	30.2	silt loam	silt
Z03	30.5	3.0	2.95×10^{-6}	6.1	62.8	31.1	silt loam	silt

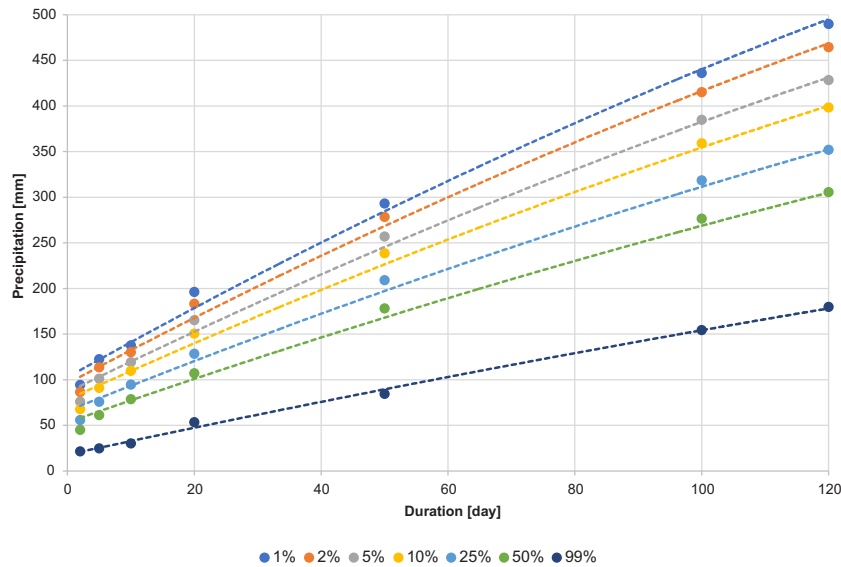


Fig. 10. Distribution of occurrence probability of maximum daily precipitation during the vegetation period, based on data from the IMGW station in Puławy from 1951 to 2020.

precipitation sum values, including different probabilities of occurrence (i.e. return periods) (Fig. 10). The depth of daily rainfall with a 100-year return period (1% occurrence probability) is slightly lower than 100 mm, similar to the maximum 24-hour rainfall values recorded in meteorological stations in the centre of Poland in the 1951–2015 period (Pińskwar et al. 2019). However, the precipitation sum values for longer periods are quite low relative to those estimated for the Nowy Wiśnicz Foothills in the northern part of the Carpathians (Demczuk et al. 2019) or even for the Lisbon Region (Vaz et al. 2018).

Slope stability calculation results

The next step of the analysis was the development of a slope model for each analysed landslide; these models were then further subjected to hydrological and geotechnical calculations, assuming the meteorological values for the years 1973–2020 as boundary conditions. As a result of these calculations, we determined the general trend of slope equilibrium condition changes, in addition to gaining insights into precipitation episodes threatening slope stability.

The calculation results (Figs 11 and 12) indicate that the average FS value for the studied objects in the years 1973–2020 reaches an increased probability of landslide occurrence ($1 < FS < 1.3$) according to Wysokiński's (1980) criteria. The lowest safety coefficient values were identified

in the autumn–winter season. Evaporation from the ground and plants is inhibited during this period. The lowest FS value occurs at the turn of March and April, associated with relatively low precipitation, largely accumulated in the form of snow cover. This results in high landslide inertia and delayed slope response to precipitation. However, at the start of the vegetation season (April), the FS increases, which is related to intensified evaporation that exceeds precipitation. In mid-May, a slight fluctuation/decrease in the FS value was observed, which is associated with an increase in precipitation sum and duration, in addition to high, stabilised infiltration of precipitation into slope cover. At the end of August and the beginning of September, the value of FS decreases rapidly due to decreasing evaporation from plants and the ground.

Analysis of slope stability during the 1973–2020 period, including the mean monthly SF values (Figs 12 and 13), indicates that slope stability is significantly correlated with seasons. The analysis shows that there is a pattern of SF fluctuation. Generally, the months at the beginning of the year are the most unfavourable from the perspective of slope stability. Also visible is a slight trend of increasing slope stability in summer months within the analysed years, which is a probable consequence of global warming.

During our analysis, we implemented 138 computational scenarios for six ravine slopes in the western part of the Nałęczów Plateau. The

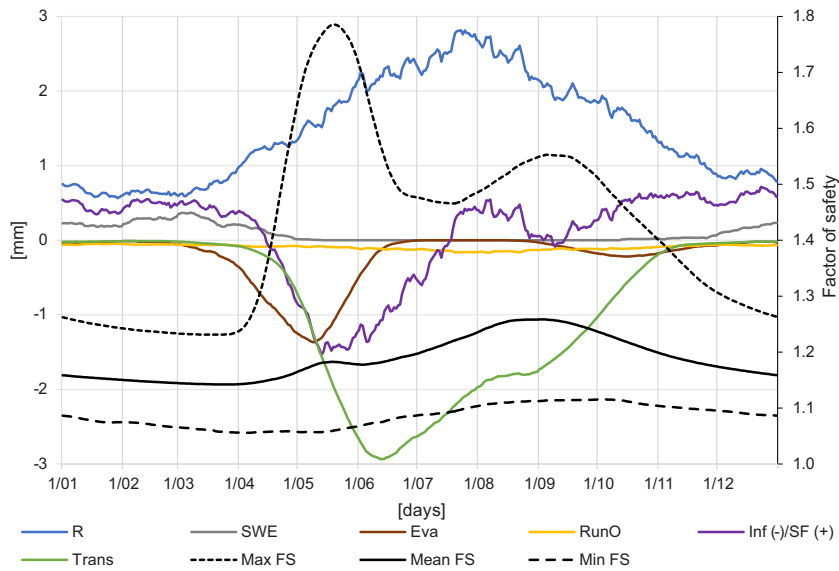


Fig. 11. Conceptual distribution of the FS against the background of annual hydrological balance components. Eva - evaporation; FS - factor of safety; Inf (-)/SF (+) - infiltration (negative values)/subsurface flow (positive values); Max FS - maximum value of the FS; Mean FS - mean value of the FS; Min FS - minimum value of the FS; R - rainfall; RunO - runoff; SWE - snow water equivalent; Trans - transpiration.

computational scenarios considered the simulated variations in the precipitation amount and its intensity (i.e. uniform, increasing or decreasing).

The critical precipitation level for landslide triggering is mainly related to the condition of the soil on the initial day of analysis (initial soil moisture content condition). The average critical precipitation level for the analysed slopes was 93.8 mm, with a minimum value of 35.2 mm,

and an average precipitation duration of about 27 days. The critical precipitation level for the wet soil is 23% lower than that for dry slopes and 19% lower than the critical precipitation level for humid soils. Increasing precipitation intensity is the most conducive factor to landslides, irrespective of initial soil moisture. This type of precipitation series allows rapid, easy infiltration into slope cover due to the precipitation intensity being

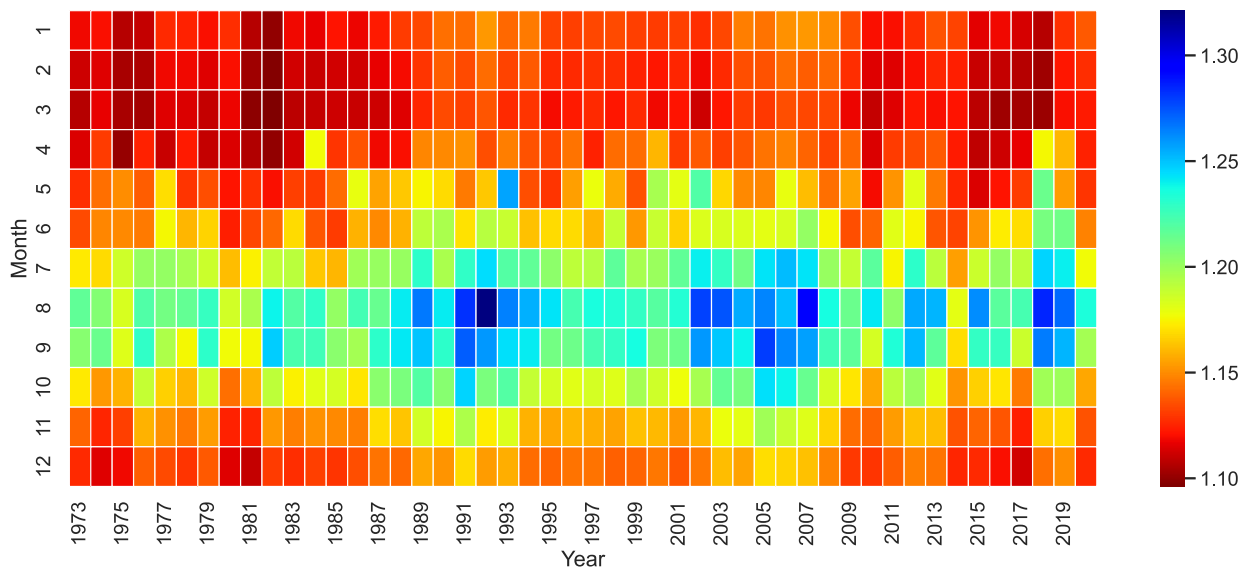


Fig. 12. Distribution of the mean value of the safety coefficient in a given month for a multiple-year period based on the selected slopes in the western part of the Nałęczów Plateau [chart generated using Matplotlib (Hunter 2007) and Seaborn (Waskom 2021) libraries in Python].

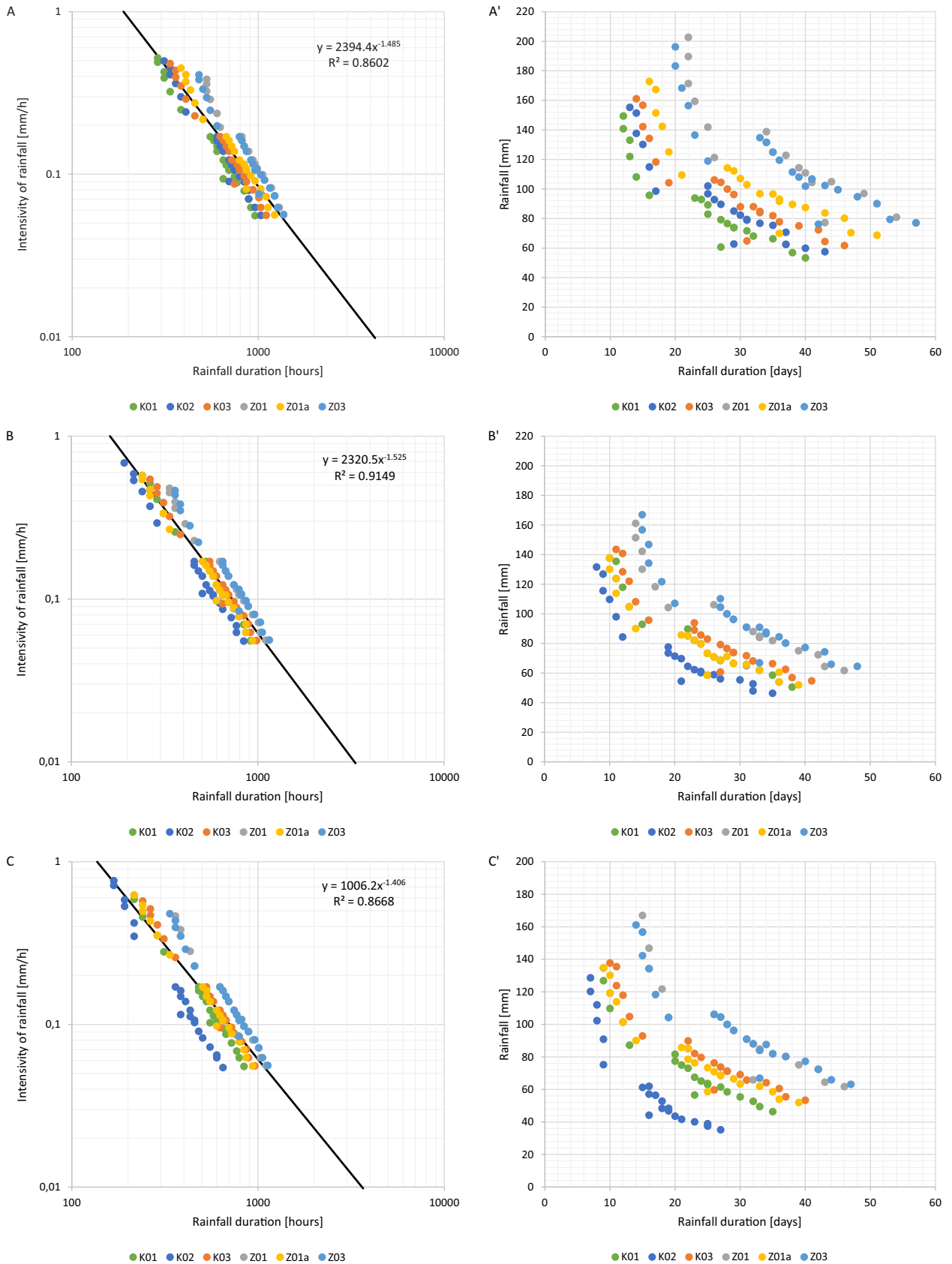


Fig. 13. Threshold precipitation values based on calculations of slope stability of the western part of the Naęczów Plateau.

Intensity-duration thresholds: A-A' - dry slope on the first analysis day; B-B' - humid slope on the first analysis day; C-C' - wet slope on the first analysis day.

Table 3. Critical precipitation level values triggering landslides in the western part of the Nałęczów Plateau in relation to initial slope cover moisture values.

Nature of precipitation	Precipitation duration			Precipitation sum			Precipitation intensity		
	Min	Mean	Max	Min	Mean	Max	Min	Mean	Max
	[days]			[mm]			[mm/h]		
Dry slope on the first analysis day									
Uniformly	23	33.0	54	57.0	98.4	138.8	0.062	0.130	0.170
Decreasing	12	20.3	43	60.7	132.9	202.7	0.075	0.311	0.519
Increasing	28	40.0	57	53.4	82.9	110.9	0.056	0.089	0.116
Humid slope on the first analysis day									
Uniformly	19	27.1	44	48.0	80.7	110.2	0.062	0.130	0.170
Decreasing	8	15.1	33	54.5	114.8	167.0	0.085	0.368	0.686
Increasing	23	33.5	48	46.4	68.1	90.9	0.055	0.087	0.115
Wet slope on the first analysis day									
Uniformly	15	25.8	44	37.5	76.6	106.1	0.062	0.130	0.170
Decreasing	7	14.3	33	44.2	112.1	167.0	0.085	0.389	0.766
Increasing	18	31.7	47	35.2	64.1	88.0	0.054	0.086	0.115

smaller than or similar to the infiltration parameters of the rocks forming the slopes. The infiltration process increases the moisture content in the slope soils and creates a saturated zone characterised by low shear strength. The table below summarises the results for the extreme and mean values of the critical (threshold) precipitation levels (Table 3).

Figure 13 shows the distribution of the obtained critical precipitation results for all the studied slopes. Notably, the (threshold) critical precipitation values shift towards the left-hand side of the plot with increasing initial soil moisture, and the spectrum of precipitation intensity data increases. The critical precipitation for landslide triggering in wet slopes is more intense, on average, than that triggering landslides in cases of dry or humid slopes. The distribution of the critical precipitation levels mainly depends on the size of the slope cover involved in the landslide process. The larger the volume (i.e. the greater the length of the slope), the greater the amount of precipitation needed over a longer time for the initiation of landslide processes.

In general, our results indicate that the precipitation levels initiating failure of the analysed slopes are low compared to threshold precipitation values reported in Polish (Gorczyca 2004, Gil, Długosz 2006) and world literature (Lumb 1975, Guzetti et al. 2007, Peruccaci et al. 2017, Marjanovic et al. 2018, Vaz et al. 2018, Teja et al. 2019, He et al. 2020). For example, for Hong Kong, Lumb (1975) reports that landslides are initiated with rainfall totals exceeding 50 mm

in the 15 days preceding the landslide events, with the principal rainfall initiating landslides (on the day of occurrence) in excess of 50 mm. Gil and Długosz (2006) report that the precipitation initiating shallow mass movements for the Carpathian area corresponds to a precipitation total of 200–250 mm for 20–40 days, whereas 100 mm of high-intensity precipitation is conducive to the formation of mudflows and combined mud–stone slides. Gorczyca's (2004) results from observations of Carpathian landslides show that such events can be initiated by smaller precipitation depths. The relationships between the values of cumulative precipitation and their duration for the analysed slopes, presented in Figure 14, demonstrate that, for the most part, the values from this study fall within the threshold ranges given for various regions. However, it should be stressed that the relationships from previous literature are empirical and usually take into account short observational periods of several days; thus, they may not be necessarily representative of all possible cases of rainfall distribution over time.

The analysis of pore pressure distribution showed that slope failure is usually related to water accumulation in the soil in the lower part of slopes, while the middle part of the slope remains unsaturated. This means that the slope instability occurs as a result of reduced suction pressure; this appears reasonable considering that the slope angle in the lower part of the slope exceeds 40°, while the internal friction angle values in loess are 30.4°–33.9° and the cohesion is close to 0 kPa. Such a relationship deviates from previous

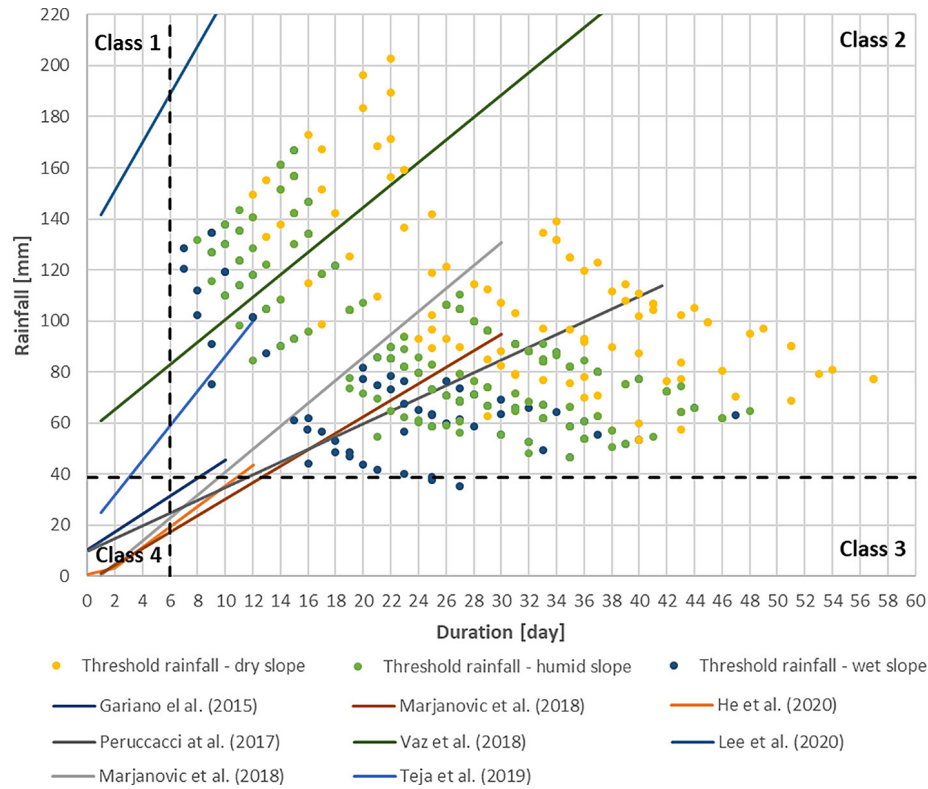


Fig. 14. Overview of the precipitation thresholds initiating landslides worldwide.

observational results and analyses of the causes of mass movements in the Carpathians (Thiel 1989, Demczuk et al. 2019), where slope failure is mostly accompanied by saturation of the whole slope with water. However, these results from the slope stability analysis for loess slopes or steep slopes indicate that, in many cases, slope failure results from a reduction in suction pressure and partial saturation of slope cover. Therefore, the precipitation levels initiating the failure of loess slopes are lower than those for the Carpathian slopes, whose inclinations are usually gentler.

A comparison of the calculation results with data on the levels of precipitation sequences for warm periods of the years 1951–2020 highlighted the sequences corresponding to Class 2, as determined by the 90th percentile for the precipitation sum and duration. However, a 2-day extension of the minimum precipitation duration (up to 8 days) is observed. Out of the 54 precipitation events classified as extreme (Class 2), only 7 coincided with the calculation results. Comparing the results obtained with those for the slopes of the Wiśnickie Foothills, calculated using the same method, the ravine slopes require, on average, half the precipitation, with a 16% shorter duration for landslide initiation.

Conclusion

Field research results indicate that the Nałęczów Plateau area is characterised by a high frequency of slope processes, including the presence of numerous landslides formed on the slopes of ravines and their anthropogenically transformed sections (i.e. sunken lanes).

The research results indicate that loess slope covers are characterised by average water permeability, relatively high internal friction angle values and low cohesion, which, combined with steep slope inclination, favours landslide formation, even when the slope is only partially saturated.

The results of deterministic analyses for the 1973–2020 period showed that the analysed slopes exhibit cyclic changes in equilibrium conditions. The most unfavourable stability conditions occur at the beginning of spring, indicating that their stability is significantly affected by snowmelt and precipitation at the onset of the vegetation season, in addition to the occurrence of episodic intense precipitation during the summer.

Deterministically calculated threshold precipitation values present a relatively wide range, thus showing a dependence on the slope moisture

conditions in the period preceding rainfall occurrence and its distribution over time. The values of cumulative precipitation initiating slope failure observed in this study fall within the range reported in the literature.

Acknowledgments

The research was financed by the National Science Center (NCN—Poland) grant no. 2020/04/X/ST10/00334.

Authors' contributions

Conceptualization: P.D. and T.Z.; Methodology: P.D. and T.Z.; Software: P.D., T.Z. and T.S.; Validation: P.D, T.Z. and T.S.; Formal analysis: P.D. and T.Z.; Investigation: P.D. and T.S.; Resources: P.D. and T.S.; Data curation: P.D., T.Z. and T.S.; Writing – original draft preparation: P.D., and T.Z.; Writing – review and editing: P.D., T.Z. and T.S.; Visualization: P.D., T.Z. and T.S.; Supervision: P.D.

All authors have read and agreed to the published version of the manuscript.

References

- Abdel-Gawad G.I., 1986. Maastrichtian non-cephalopod mollusks (Scaphopoda, Gastropoda and Bivalvia) of the Middle Vistula Valley, Central Poland. *Acta Geologica Polonica* 36: 69–224.
- Abraham M.T., Satyasm N., Pradhan B., Segoni S., Alamri A., 2021. Developing a prototype landslide early warning system for Darjeeling Himalayas using SIGMA model and real-time field monitoring. *Geosciences Journal*. DOI 10.1007/s12303-021-0026-2.
- Banasik K., Wałęga A., Węglarczyk S., Więzik B., 2017. Aktualizacja metodyki obliczania przepływów i opadów maksymalnych o określonym prawdopodobieństwie przewyższenia dla zlewni kontrolowanych i niekontrolowanych oraz identyfikacji modeli transformacji opadu w odpływ. Stowarzyszenie Hydrologów Polskich, Warszawa.
- Borecka A., Kaczmarczyk R., 2007. Geologiczno-inżynierska ocena zagrożeń osuwiskowych w utworach lessowych południowo-wschodniej Polski. *Geologos* 11: 347–356.
- Calvello M., d'Orsi R.N., Piciullo L., Paes N., Magalhaes M., Lacerda W.A., 2015. The Rio de Janeiro early warninh system for rainfall-induced landslides: Analysis pf performance for the years 2010–2013. *International Journal of Disaster Risk Reduction* 12: 3–15.
- Chae B.G., Park H.J., Catani F., Simoni A., Berti M., 2017. Landslide prediction, monitoring and early warning: A concise review of state-of-the-art. *Geosciences Journals* 21(6): 1033–1070. DOI 10.1007/s12303-017-0034-4.
- Chomicz K., 1951. Ulewy i deszcze nawalne w Polsce, *Wiadomości Służby Hydrologicznej i Meteorologicznej* 3: 5–88.
- Demczuk P., Zydrón T., Siłuch M., 2019. Rainfall thresholds for the occurrence of shallow landslides determined for slopes in the Nowy Wiśnicz Foothills (Polish Flysch Carpathians). *Geological Quarterly* 63(4): 822–838.
- Dziewiański J., Wota A.K., Limanówka D., Cebulak E., Michalik S., 2004. Katastrofalny spływ wodno-gliniasty w Muszynie w lipcu 2002 roku. Wydawnictwo Instytutu Gospodarki Surowcami Mineralnymi i Energią PAN, Kraków.
- Gariano S.L., Brunetti M.T., Iovine G., Melillo M., Peruccacci S., Terranova O., Vennari C., Guzzetti F., 2015. Calibration and validation of rainfall thresholds for shallow landslide forecasting in Sicily, southern Italy. *Geomorphology* 228: 653–665.
- Gariano S.L., Guzzetti F., 2016. Landslides in a changing climate. *Earth-Science Reviews* 162: 227–252.
- German K., 1998. Przebieg wezbrania i powodzi 9 lipca 1997 roku w okolicach Żegociny oraz ich skutki w krajobrazie. In: Starkel L., Grela J. (eds), *Powódź w dorzeczu górnej Wisły w lipcu 1997 roku*, Konferencja Naukowa, Kraków, 7-9 maja 1998 roku Oddz. PAN, Kraków: 177-184.
- Gil E., Długosz M., 2006. Threshold values of rainfalls triggering selected deep-seated landslides in the Polish Flysch Carpathians. *Studia Geomorphologica Carpatho-Balcanica* 40: 21–43.
- Gorczyca E., 2004. *Przekształcanie stoków fliszowych przez procesy masowe podczas katastrofalnych opadów (dorzecze Łososiny)*. Wydawnictwo Uniwersytetu Jagiellońskiego, Kraków.
- Guzzetti F., Peruccacci S., Rossi M., Stark C.P., 2007. Rainfall thresholds for the initiation of landslides in central and southern Europe. *Meteorology and Atmospheric Physics* 98: 239–267. DOI 10.1007/s00703-007-0262-7.
- Harasimiuk M., 1980. *Rzeźba strukturalna Wyżyny Lubelskiej i Roztocza*. Rozprawa habilitacyjna. Wydawnictwo UMCS, Lublin: 136.
- Harasimiuk M., Henkiel A., 1975/1976. Wpływ budowy geologicznej i rzeźby podłoża na ukształtowanie pokrywy lessowej w zachodniej części Płaskowyżu Nałęczowskiego. *Annales UMCS sectio B*, 30/31, Lublin, 55–80.
- Harasimiuk M., Henkiel A., 1976. Osobliwości pokrywy lessowej zachodniej części Płaskowyżu Nałęczowskiego (Peculiarities of the loess cover in the western part of the Nałęczów Plateau). *Bulletin of the Geological Institution* 297: 177–184.
- Harasimiuk M., Henkiel A., 1978. Wpływ budowy geologicznej i rzeźby podłoża na ukształtowanie pokrywy lessowej w zachodniej części Płaskowyżu Nałęczowskiego. *Annales UMCS sectio B* 30/31: 55–80.
- Harasimiuk M., Jezierski W., 1998. Północna krawędź Wyżyny Lubelskiej w okolicy Skowieszyna. In: Dobrowolski R. (ed.), *Główne kierunki badań geomorfologicznych w Polsce. Stan aktualny i perspektywy. IV Zjazd Geomorfologów Polskich. III. Przewodnik wycieczkowy*. Wydawnictwo UMCS, Lublin: 169–173.
- Harasimiuk M., Rodzik J., Zgłobicki W., 2000. The role of mass-movements in development of gullies in loess areas of the Lublin Upland (SE Poland). In: *Book of Abstracts of International Symposium on "Gully Erosion under Global Change"*, Leuven, Belgium, 16–19 April 2000: 72.
- He S., Wang J., Liu S., 2020. Rainfall event-duration thresholds for landslide occurrences in China. *Water* 12: 494. DOI 10.3390/w12020494.
- Henkiel A., Nitychoruk J., 1983. Spękania ciosowe i drobne struktury tektoniczne w skałach kredowo-paleoceńskich północno-zachodniej części Wyżyny Lubelskiej. *Annales UMCS sectio B* 35/36: 13–27.

- Higgins J.D., Modeer V.A., Jr. 1996. Loess. In: Turner K.A., Schuster R. (eds), *Landslides – investigation and mitigation. Special Report 247*. National Academy Press, Washington, USA.
- Hunter D., 2007. Matplotlib: A 2D Graphics Environment. *Computing in Science & Engineering*, 9 (3), 90–95. In: *Heifangtai platform, North-West China. Environmental Earth Sciences* 66: 1707–1713.
- Kaczmarczyk R., Tchórzewska S., Woźniak H., 2011. Charakterystyka wybranych osuwisk z terenu południowej Polski uaktywnionych po okresie intensywnych opadów w 2010 roku. *Biuletyn Państwowego Instytutu Geologicznego* 446(1): 65–73.
- Kaczorowska Z., 1962. Opady w Polsce w przekroju wieloletnim. *Prace Geograficzne*, 33: 70–74.
- Kaszewski B.M., 2008. Klimat. In: Uziak S., Turski R. (eds), *Środowisko przyrodnicze Lubelszczyzny*. Lubelskie Towarzystwo Naukowe, Lublin: 75–112.
- Kaszewski B. M., Siwek K., 2005. Dobowe sumy opadu atmosferycznego ≥ 50 mm w dorzeczu Wieprza i ich uwarunkowania cyrkulacyjne (1951–2000), In: Bogdanowicz E., Kossowska-Cezak U., Szkutnicki J. (eds), *Ekstremalne zjawiska hydrologiczne i meteorologiczne*. IMGW: 325–335.
- Kęsik A., 1961. Valles des terrains loessiques de la partie Ouest du Plateau de Nałęczów. *Annales UMCS sectio B XV*: 123–153.
- Lee W.Y., Park S.K., Sung H.H., 2020. The optimal rainfall thresholds and probabilistic rainfall conditions for a landslide early warning system for Chuncheon, Republic of Korea. *Landslides*. DOI 10.1007/s10346-020-01603-3.
- Leng X., Wang C., Zhang J., Sheng Q., Cao S., Chen J., 2021. Deformation Development Mechanism in a Loess Slope With Seepage Fissures Subjected to Rainfall and Traffic Load. *Frontiers Earth Science, Geohazards and Georisks* 9:769257. DOI 10.3389/feart.2021.769257.
- Lorenc H., Cebulak E., Głowicki B., Kowalewski M., 2012. Struktura występowania intensywnych opadów deszczu powodujących zagrożenie dla społeczeństwa, środowiska i gospodarki Polski. In: Lorenc H. (ed.), *Kłęski żywiołowe a bezpieczeństwo kraju*. Monografie IMGW-PIB: 7–32.
- Lumb P., 1975. Slope failure in Hong Kong. *Quarterly Journal of Engineering Geology and Hydrogeology* 8: 31–65.
- Machalski M., 2005. Late Maastrichtian and earliest Danian scaphitid ammonites from central Europe: Taxonomy, evolution, and extinction. *Acta Palaeontologica Polonica* 50: 653–696.
- Marjanovic M., Krautblatter M., Abolmasov B., Duric U., Sandic C., Nikoic V., 2018. The rainfall-induced landsliding in Western Serbia: A temporal prediction approach using Decision Tree technique. *Engineering Geology* 232: 147–159.
- Maruszczak H., 1973. Erozja wąwozowa we wschodniej części pasa wyżyn południowopolskich. *Zeszyty Problemowe Postępów Nauk Rolniczych* 151: 15–30.
- Maruszczak H., 1986. Tendencje sekularne i zjawiska ekstremalne w rozwoju rzeźby małopolskich wyżyn lessowych w czasach historycznych. *Czasopismo Geograficzne* 57(2): 271–282.
- Maruszczak H., 1991. Zróznicowanie stratygraficzne lessów w Polsce. In: Maruszczak H. (ed.), *Podstawowe profile lessów w Polsce*. Wydawnictwo UMCS, Lublin: 13–35.
- Maruszczak H., Trembaczowski J., 1958. Geomorfologiczne skutki gwałtownej ulewy w Piaskach Szlacheckich koło Krasnegostawu, *Annales UMCS sectio B* 11: 129–160.
- Mularz S., Rybicki S., 1999. Geologiczno-inżynierskie uwarunkowania deformacji terenu i szkód budowlanych w staromiejskiej dzielnicy Sandomierza. *Przegląd Geologiczny* 47: 1117–1124.
- Oszczypko N., Golonka J., Zuchiewicz W., 2002. Osuwisko w Lachowicach (Beskidy Zachodnie): skutki powodzi z 2001 r. *Przegląd Geologiczny* 50(10/1): 893–898.
- Parczewski W., 1960. Warunki występowania nagłych wezbrań na małych ciekach. *Wiadomości Służby Hydrologicznej i Meteorologicznej* 8(3): 83–155.
- Peruccacci S., Brunetti M.T., Gariano S.L., Melillo M., Rossi M., Guzzetti F., 2017. Rainfall thresholds for possible landslide occurrence in Italy. *Geomorphology* 290: 39–57.
- Pińskwar L., Choryński A., Graczyk D., Kundzewicz Z.W., 2019. Observed changes in extreme precipitation in Poland: 1991–2015 versus 1961–1990. *Theoretical and Applied Climatology* 135: 773–787. DOI 10.1007/s00704-018-2372-1.
- Poprawa D., Rączkowski W., 1998. Geologiczne skutki powodzi 1997 na przykładzie osuwisk województwa nowosądeckiego. In: Starkel L., Grela J. (eds), *Powódź w dorzeczu górnej Wisły*. Wydawnictwo PAN, Kraków: 119–131.
- Poprawa D., Rączkowski W., 2003. Osuwiska Karpat. *Przegląd Geologiczny* 51(8): 685–692.
- Pożaryska K., 1967. Badania warstw pogranicznych kredy i trzeciorzędu w Polsce pozakarpaciej. *Kwartalnik Geologiczny*, t. 11, z. 3, Warszawa.
- Pożaryski W., 1948. Jura i kreda między Radomiem, Zawichostem i Kraśnikiem. *Poland Institute of Geology Bulletin* 46: 1–141.
- Pożaryski W., Maruszczak H., Lindner L., 1994. Chronostratygrafia osadów plejstocenijskich i rozwój doliny Wisły środkowej ze szczególnym uwzględnieniem przełomu przez wyżyny południowopolskie. *Prace Państwowego Instytutu Geologicznego* 147, Warszawa.
- Rączkowski W., Mrozek T., 2002. Activating of landsliding in the Polish Flysch Carpathians by the end of the 20th century. *Studia Geomorphologica Carpatho-Balcanica* XXXVI: 91–111.
- Rodzic J., Ciupa T., Janicki G., Kociuba W., Tyc A., Zglobicki W., 2008. Współczesne przemiany rzeźby Wyżyn Polskich. In: Starkel L., Kostrzewski A., Kotarba A, Krzemień K. (eds), *Współczesne przemiany rzeźby Polski*. SGP, IGiP UJ, Kraków: 165–214.
- Rodzic J., Janicki G., 2003. Local downpours and their erosional effects. *Papers on Global Change IGBP* 10: 49–66.
- Rodzic J., Janicki G., Zagórski P., Zglobicki W., 1998. Deszcze nawalne na Wyżynie Lubelskiej i ich wpływ na rzeźbę obszarów lessowych. *Dokumentacja Geograficzna IGiPZ PAN* 11: 45–68.
- Rybicki S., Margielewski W., Domagała A., 1998. Osuwisko na stoku góry Palenica w Szczawnicy (pieniński pas skalowy) i jego związek z ekstremalnymi opadami w lipcu 1997 r. *Przegląd Geologiczny* 46(11): 1162–1170.
- Segoni S., Rosi A., Rossi G., Catani F., Casagli N., 2014. Analysing the relationship between rainfalls and landslides to define a mosaic of triggering thresholds for regional-scale warning systems. *Natural Hazards Earth System Science* 14: 2637.
- Shi W., Li Y., Zhang W., Liu J., He S., Mo P., Guan F., 2020. The loess landslide on 15 March 2019 in Shanxi Province, China. *Landslides* 17: 677–686. DOI 10.1007/s10346-019-01342-0.

- Siwek K., 2006. *Zróżnicowanie opadów atmosferycznych na Lubelszczyźnie w latach 1951–2000*, praca doktorska, Archiwum Biblioteki Głównej UMCS, Lublin.
- Starkel L., 1986. Rola zjawisk ekstremalnych i procesów sekwencyjnych w ewolucji rzeźby (na przykładzie fliszowych Karpat). *Czasopismo Geograficzne* 57(2): 203–213.
- Starkel L., 1996. Geomorphic role of extreme rainfalls in the Polish Carpathians, *Studia Geomorphologica Carpatho-Balcanica* 30: 21–38.
- Starkel L., 1997. Mass movement during the Holocene: Carpathian example and the European perspective. *Palaeoclimate Research* 19: 385–400.
- Starkel L., 2008. Rola ekstremalnych zjawisk meteorologicznych w przekształcaniu rzeźby południowej Polski. In: Kotarba M. J. (ed.), *Przemiany środowiska naturalnego a rozwój zrównoważony*. Wydawnictwo TBPŚ GEOSFERA, Kraków: 41–52.
- Szalińska W., Otop I., 2012. Ocena struktury czasowo-prze-strzennej opadów z wykorzystaniem wybranych wskaźników do identyfikacji zdarzeń ekstremalnych. *Woda-Środowisko-Obszary Wiejskie*, T. 12, z. 2.
- Teisseyre A. K., 1994. *Spytyw stokowy i współczesne osady deluwialne w lessowym rejonie Henrykowa na Dolnym Śląsku*. Wydawnictwo Uniwersytetu Wrocławskiego, Wrocław.
- Teja T. S., Dikshit A., Satyam N., 2019. Determination of rainfall thresholds for landslide prediction using an algorithm-based approach: Case study in the Darjeeling Himalayas. *India. Geosciences* 9: 302. DOI 10.3390/geosciences9070302.
- Thiel K. (ed.), 1989. *Kształtowanie fliszowych stoków karpacckich przez ruchy masowe na przykładzie badań na stoku Bystrzyca w Szymbarku*. Wydawnictwo IBW PAN, Gdańsk.
- Tu X. B., Kwong A. K. L., Dai F. C., Tham L. G., Min H., 2009. Field monitoring of rainfall infiltration in a loess slope and analysis of failure mechanism of rainfall-induced landslides. *Engineering Geology* 105: 134–150.
- Vaz T., Zezere J.L., Pereira S., Oliveira S.C., Garcia R.A.C., Quaresma I., 2018. Regional rainfall thresholds for landslide occurrence using a centenary database. *Natural Hazards and Earth System Sciences* 18: 1037–1054. DOI 10.5194/nhess-18-1037-2018.
- Waskom M.L., 2021. Seaborn: Statistical data visualization. *The Journal of Open Source Software* 6(60): 3021. DOI 10.21105/joss.03021.
- Wojciechowski T., 2019. Podatność osuwiskowa Polski. *Prze-gląd Geologiczny* 67: 320–325. DOI 10.7306/2019.25.
- Wysokiński L., 1980. Kryterium dynamiki zbroczy. *Biuletyn Instytutu Geologicznego* 324.
- Wysokiński L., 2011. Metody prognozowania i zabezpieczania osuwisk. XXV Konferencja Naukowo Techniczna *Awarie budowlane 2011*, 2–27 May 2011: 291–320.
- Chen X.-L., Liu C.-G., Chang Z.-F., Zhou Q., 2016. The relationship between the slope angle and the landslide size derived from limit equilibrium simulations. *Geomorphology* 253: 547–550.
- Xie W.-I., Gu Q., Wu J.Y., Li P., Yang H., Zhang M., 2021. Analysis of loess landslide mechanism and numerical simulation stabilization on the Loess Plateau in Central China. *Natural Hazards* 106: 805–827. DOI 10.1007/s11069-020-04492-w.
- Xing X., Li T., Fu Y., 2016. Determination of the related strength parameters of unsaturated loess with conventional triaxial test. *Environmental Earth Sciences* 75: 82. DOI 10.1007/s12665-015-4797-5.
- Xu C., Xu X.W., Zheng W.J., Wei Z.Y., Tan X.B., Han Z.J., Li C.Y., Liang M.J., Li Z.Q., Wang H., Wang M.M., Ren J.J., Zhang S.M., He Z.T., 2013. Landslides triggered by the April 20, 2013. Lushan, Sichuan Province Ms7.0 strong earthquake of China. *Seismology and Geodynamics* 35(3): 45–55.
- Xu L., Coop M.R., Zhang M., Wang G., 2018. The mechanics of a saturated silty loess and implications for landslides. *Engineering Geology* 236: 29–42.
- Xu L., Dai F.C., Gong, Q.M., Tham, L.G., Min, H., 2012. Irrigation-induced loess flow failure in Heifangtai Platform, North-West China. *Environmental Earth Sciences* 66: 1707–1713.
- Yates K., Fenton C.H., Bell D.H., 2018. A review of the geotechnical characteristics of loess and loess-derived soils from Canterbury, South Island, New Zealand. *Engineering Geology* 236(26): 11–21.
- Żarski M., 1988. *Objaśnienia do Szczegółowej mapy geologicznej Polski 1: 50 000, arkusz Puławy*. Wydawnictwa Geologiczne.
- Żarski M., Jakubowski G., Gawor-Biedowa E., 1998. The first Polish find of Lower Paleocene crocodile *Thoracosaurus Leidy, 1852*: Geological and paleontological description. *Kwartalnik Geologiczny* 42: 141–160.
- Zhou Y.F., Tham L.G., Yan R.W. M., Xu L., 2014. The mechanism of soil failures along cracks subjected to water infiltration. *Computers and Geotechnics* 55: 330–341.
- Zhu Y., Qiu H., Yang D., Liu Z., Ma S., Pei Y., He J., Du C., Sun H., 2021. Pre- and post-failure spatiotemporal evolution of loess landslides: A case study of the Jianguou landslide in Ledu, China. *Landslides*. DOI 10.1007/s10346-021-01714-5.